PLOS ONE

RESEARCH ARTICLE

Downregulation of *COL12A1* and *COL13A1* by a selective EP2 receptor agonist, omidenepag, in human trabecular meshwork cells

Masashi Kumon[1☯], Masahiro Fuwa[1☯*], Atsushi Shimazaki[1], Noriko Odani-Kawabata[2], Ryo Iwamura[3], Kenji Yoneda[3], Masatomo Kato[1]

1 Product Development Division, Santen Pharmaceutical Co., Ltd., Nara, Japan, **2** Product Development Division, Santen Pharmaceutical Co., Ltd., Osaka, Japan, **3** Pharmaceutical Division, Pharmaceuticals Research Laboratory, UBE Corporation, Yamaguchi, Japan

☯ These authors contributed equally to this work.
* masahiro.fuwa@santen.com

Citation: Kumon M, Fuwa M, Shimazaki A, Odani-Kawabata N, Iwamura R, Yoneda K, et al. (2023) Downregulation of *COL12A1* and *COL13A1* by a selective EP2 receptor agonist, omidenepag, in human trabecular meshwork cells. PLoS ONE 18(1): e0280331. https://doi.org/10.1371/journal.pone.0280331

Editor: Ted S. Acott, Oregon Health and Science University, UNITED STATES

Received: June 14, 2022

Accepted: December 27, 2022

Published: January 11, 2023

Data Availability Statement: All relevant data are within the paper and its Supporting Information files.

Funding: M. Kumon, M.F., A.S., N.O.K., and M. Kato are employees of Santen Pharmaceutical Co., Ltd. R.I. and K.Y. are employees of UBE Corporation. The funders provided support in the form of salaries for authors M. Kumon, M.F., A.S., N.O.K., M. Kato, R.I., and K.Y. but did not have any additional role in the study design, data collection

Abstract

Omidenepag isopropyl (OMDI) is an intraocular pressure (IOP)-lowering drug used to treat glaucoma. The active form of OMDI, omidenepag (OMD), lowers elevated IOP, the main risk factor for glaucoma, by increasing the aqueous humor outflow; however, a detailed understanding of this mechanism is lacking. To clarify the IOP-lowering mechanism of OMDI, the effects of OMD on the mRNA expression of the extracellular matrix, matrix metalloproteinases (MMPs), and tissue inhibitors of metalloproteinases (TIMPs) were evaluated in human trabecular meshwork cells. Under 2D culture conditions, the mRNA expression of *FN1*, *COL1A1*, *COL1A2*, *COL12A1*, and *COL13A1* decreased in a concentration-dependent manner after 6 or 24 h treatment with 10 nM, 100 nM, and 1 μM OMD, while that of *COL18A1* decreased after 6 h treatment with 1 μM OMD. Significant changes in expression were observed for many MMP and TIMP genes. Under 3D culture conditions, the extracellular matrix-related genes *COL12A1* and *COL13A1* were downregulated by OMD treatment at all three concentrations. Under both 2D and 3D culture conditions, *COL12A1* and *COL13A1* were downregulated following OMD treatment. Reduction in the extracellular matrix contributes to the decrease in outflow resistance, suggesting that the downregulation of the two related genes may be one of the factors influencing the IOP-lowering effect of OMDI. Our findings provide insights for the use of OMDI in clinical practice.

Introduction

Glaucoma, the leading cause of irreversible blindness, is an ocular neurodegenerative disease characterized by selective loss of retinal ganglion cells resulting in progressive visual field defects [1–4]. The only evidence-based treatment for glaucoma is intraocular pressure (IOP) reduction [5–7]. Prostaglandin F (FP) receptor agonists are mainly used as first-line treatment agents for glaucoma [8,9]; however, they are occasionally associated with the topical ocular side effect of prostaglandin-associated periorbitopathy (PAP), which may limit their clinical use [10–12]. Therefore, alternative treatment options with better safety profiles and novel mechanisms of action are needed.

and analysis, decision to publish, or preparation of the manuscript.

Competing interests: Competing Interests Statement: All authors declare no non-financial competing interests. Their commercial affiliation to Santen Pharmaceutical Co., Ltd. and UBE Corporation does not alter their adherence to PLOS ONE policies on sharing data and materials.

Omidenepag isopropyl (OMDI) is the first prostaglandin E_2 receptor EP2 subtype (EP2 receptor) agonist used as an IOP-lowering drug for glaucoma treatment worldwide, approved in Japan in 2018, followed by Korea and other Asian countries [13,14]. OMDI exerts potent IOP-lowering effects in both animals [15,16] and humans [17–19]. OMDI ophthalmic solution of 0.002% has been used for the treatment of glaucoma and ocular hypertension [13,14]. OMDI is a prodrug that improves the corneal permeability of omidenepag (OMD), the active form of OMDI, which has a novel non-prostaglandin chemical structure that differs from that of any existing prostaglandin analog, including FP receptor agonists, and highly selective EP2 receptor agonist activity [20]. A multicenter, double-blinded, controlled phase 3 clinical study (AYAME Study [NCT02623738]) [18] demonstrated that OMDI is safe and tolerable and has noninferior IOP-lowering efficacy comparable to that of latanoprost, the FP receptor agonist. In addition to monotherapy, we previously demonstrated that OMDI exerted additive IOP-lowering effects when combined with timolol (β-adrenergic antagonist), brinzolamide (carbonic anhydrase inhibitor), netarsudil and ripasudil (Rho-associated coiled-coil containing protein kinase inhibitor), or brimonidine (α_2-adrenergic agonist), in conscious ocular normotensive monkeys [16]. Furthermore, unlike FP receptor agonists, previous nonclinical studies have suggested that OMDI does not cause PAP [21,22]. Considering its mechanism of action, which involves stimulating the EP2 receptor followed by increasing the aqueous humor outflow through both conventional and uveoscleral outflow pathways [23], IOP-lowering efficacy, and safety, OMDI is a potential alternative first-line therapeutic agent to FP receptor agonists.

IOP is regulated by resistance to aqueous humor outflow caused by the extracellular matrix (ECM) within the deepest portion of the trabecular meshwork (TM) and basement lamina of the Schlemm's canal (SC) inner wall endothelium [24–26]. Elevated IOP is the only validated risk factor for glaucoma [6,27]; hence, IOP reduction remains the primary goal of therapy [5,7]. The main reason for the elevated IOP in primary open-angle glaucoma, the major subtype of glaucoma, is increased resistance in the conventional outflow pathway consisting of the TM and SC [24]. We previously demonstrated that OMDI lowers IOP by increasing the aqueous humor outflow through both the conventional and uveoscleral outflow pathways in ocular hypertensive monkeys [23].

This mechanism of action is unique to OMDI because the FP receptor agonists and the other EP2 receptor agonist butaprost with prostaglandin structure and broad affinity to other prostanoid receptors predominantly stimulate the uveoscleral outflow pathway [28,29]. Although OMD can modulate TM cell fibrosis and SC endothelial cell permeability [30], a detailed understanding of the molecular mechanism of action of OMDI facilitating aqueous humor outflow is lacking. Thus, to clarify the IOP-lowering mechanism of OMDI, especially focusing on the conventional outflow pathway, we evaluated the effects of OMD on the mRNA expression of the ECM, matrix metalloproteinases (MMPs), and tissue inhibitors of metalloproteinases (TIMPs) associated with aqueous humor outflow resistance [24–26] using quantitative real-time PCR in two- and three-dimensionally (2D and 3D) cultured human TM (HTM) cells. Clarification of the mechanism of OMDI in the conventional outflow pathway provides reference information for determining the order of drug use initiation combined with existing anti-glaucoma drugs, which will lead to more effective use in clinical practice.

Materials and methods

Materials

OMD was synthesized by UBE Corporation (Yamaguchi, Japan) and dissolved in dimethyl sulfoxide (DMSO [Nacalai Tesque, Kyoto, Japan]).

Culture of primary human trabecular meshwork (HTM) cells

Primary HTM cells were obtained from ScienCell Research Laboratories (Carlsbad, CA, USA). HTM cells were isolated from a single donor. To characterize these HTM cells, we confirmed myocilin (MYOC) upregulation induced by dexamethasone (DEX) treatment according to the procedure described in previous reports [31–34] (S1 Fig). HTM cells were maintained in the supplemented manufacturer-specified medium, namely, trabecular meshwork cell medium (TMCM) containing 2% fetal bovine serum, the manufacturer-specified supplement (i.e., undisclosed growth factors, hormones, and proteins), 100 units/mL of penicillin, and 100 μg/mL of streptomycin (ScienCell Research Laboratories). HTM cells were cultured in a poly-L-lysine-coated flask, and the supplemented TMCM was exchanged every 3–4 d. HTM cells were used between passages 3 and 5 in the present study.

In vitro cell viability assay

HTM cells were seeded in 96-well plates pre-coated with poly-L-lysine (AGC Techno Glass Co., Ltd., Shizuoka, Japan) at a density of 1.0×10^4 cells/well. The cells were placed in a 5% CO_2 incubator at 37˚C and cultured in supplemented TMCM. The HTM cells reached confluence at 24 h after seeding, following which, the supplemented TMCM was removed and the cells were washed once with non-supplemented TMCM. The cells were incubated for 24 h with OMD at 10 nM, 100 nM, and 1 μM in non-supplemented TMCM containing 0.1% DMSO, while non-supplemented TMCM containing 0.1% DMSO was used as the vehicle, and the cell viability was assessed using 3-(4,5-dimethylthiazol-2-yl)-5-(3-carboxymethoxyphenyl)-2-(4-sulfophenyl)-2H-tetrazolium (MTS) assays in accordance with the manufacturer's instructions (CellTiter 96 AQ_{ueous} One Solution Cell Proliferation Assay, Promega, Madison, WI, USA).

Drug treatment of 2D- and 3D-cultured HTM cells

For the 2D culture, HTM cells were seeded in supplemented TMCM in 12-well plates pre-coated with poly-L-lysine (AGC Techno Glass Co., Ltd., Shizuoka, Japan) at a density of 1.2×10^5 cells/well. The HTM cells reached confluence at 24 h after seeding. Subsequently, the supplemented TMCM was removed and the confluent cells were washed once with non-supplemented TMCM. The cells were treated with OMD at 10 nM, 100 nM, and 1 μM in non-supplemented TMCM containing 0.1% DMSO for 6 or 24 h, while non-supplemented TMCM, containing 0.1% DMSO was used as the vehicle.

For the 3D tissue generation, a 3D culture of HTM cells was performed according to a previous study [35], with modifications. Briefly, HTM cells were suspended in Tris-buffered saline containing 150 mM sodium chloride and 0.04 mg/mL gelatin (Wako Pure Chemicals, Osaka, Japan) with gentle shaking for 30 min at approximately 20–25˚C. The cells were briefly centrifuged at 500–600 g and resuspended in supplemented TMCM. The cells were then seeded in 24-well plate cell culture inserts (0.4-μm transparent PET membrane; Corning, Corning, NY, USA) coated with 0.12 mg/mL fibronectin (Sigma-Aldrich, Saint Louis, MO, USA) at a density of 5.0×10^5 cells/well. To generate stable 3D-cultured tissues that exhibit strong three-dimensional cell–cell adhesion, the HTM cells were cultured in supplemented TMCM for 6 d. Subsequently, the supplemented TMCM was removed, and the cells were washed once with non-supplemented TMCM. The cells were treated with OMD at 10 nM, 100 nM, and 1 μM in non-supplemented TMCM containing 0.1% DMSO, for 6 or 24 h, while non-supplemented TMCM containing 0.1% DMSO was used as the vehicle.

RNA extraction, reverse transcription, and quantitative real-time PCR

After 6 and 24 h of OMD treatment, total RNA was extracted from the 2D- and 3D-cultured HTM cells using RNeasy Plus Universal Mini Kit (Qiagen, Hilden, Germany) in accordance with the manufacturer's instructions. For the reverse transcription and quantitative real-time PCR, the experiment was performed as previously described [36,37], with minor modifications. Briefly, total RNA was used for reverse transcription to synthesize complementary DNA (cDNA) by means of QuantiTect Reverse Transcription kit (Qiagen) in accordance with the manufacturer's instructions. Real-time PCR was performed using either the Mx3005P Real-Time PCR System (Agilent Technologies, Santa Clara, CA, USA) with QuantiFast SYBR Green PCR Kit (Qiagen) or the QuantStudio 3 Real-Time PCR System (Thermo Fisher Scientific) with PowerUp SYBR Green Master Mix (Thermo Fisher Scientific) in accordance with the manufacturers' instructions. The expression of each gene was determined by the standard ΔΔCt method. The relative expression level of target genes (*FN1*, *COL1A1*, *COL1A2*, *COL4A2*, *COL12A1*, *COL13A1*, *COL18A1*, *MMP1*, *MMP2*, *MMP3*, *MMP9*, *MMP11*, *MMP12*, *MMP14*, *MMP15*, *MMP16*, *MMP17*, *MMP24*, *TIMP1*, *TIMP2*, *TIMP3*, and *TIMP4*) was normalized to that of *GAPDH* and presented as percentages relative to the vehicle-treated group. Some of the pre-designed primers were purchased from Takara Bio (Shiga, Japan). The sequences of the primers or part numbers of the pre-designed primers for the evaluated genes are shown in Table 1.

Table 1. Primers used for quantitative real-time PCR.

Gene	Primer set P/N	Forward (5′–3′)	Reverse (5′–3′)
GAPDH	HA067812	-	-
FN1	-	AGCGGACCTACCTAGGCAAT	GGTTTGCGATGGTACAGCTT
COL1A1	-	GAGAGCATGACCGATGGATT	CCTTCTTGAGGTTGCCAGTC
COL1A2	-	GAGGGCAACAGCAGGTTCACTTA	TCAGCACCACCGATGTCCAA
COL4A2	-	CCACAGTCAGGATGTCTCCATC	CGGTGACACCAGTGATTGGC
COL12A1	-	CCACAGGTTCAAGAGGTCCC	TGTGTTAGCCGGAACCTGGA
COL13A1	HA144155	-	-
COL18A1	-	GGCACGCATCTTCTCCTTT	CACGATGTAGGCGTGATGG
MMP1	HA169158	-	-
MMP2	HA173965	-	-
MMP3	HA160220	-	-
MMP9	HA129244	-	-
MMP11	HA154311	-	-
MMP12	HA122565	-	-
MMP14	HA274826	-	-
MMP15	HA125534	-	-
MMP16	HA250859	-	-
MMP17	HA153284	-	-
MMP24	HA269320	-	-
TIMP1	HA257212	-	-
TIMP2	HA143999	-	-
TIMP3	HA269773	-	-
TIMP4	HA157583	-	-

Primer sets with P/N were pre-designed and purchased from Takara Bio (Shiga, Japan). Other primers' sequences are shown.

https://doi.org/10.1371/journal.pone.0280331.t001

Statistical analysis

Each value depicted in the figures represents the mean ± S.E. All statistical analyses were performed using EXSUS software version 10.0.7 (EP Croit, Tokyo, Japan) in accordance with the manufacturer's instructions. For *in vitro* cell viability assay, Bartlett's test for equal variance was performed followed by Dunnett's test for multiple comparisons in parametric method. For quantitative real-time PCR analysis, after Bartlett's test for equal variance, Dunnett type multiple comparisons were performed in the following manner: (a) If the data were non-equal variance ($P < 0.05$), the data were calculated using the parametric method following Log transformation; (b) In the case of equal variance ($P \geq 0.05$), the parametric method was used. Differences were considered significant at $P < 0.05$.

Results

Effect of OMD on HTM cell viability

To determine whether OMD has cytotoxicity in HTM cells, we first examined the effect of OMD at concentrations of 10 nM, 100 nM, and 1 μM for 24 h on cell viability under 2D culture conditions. Fig 1A shows no changes in the appearance of HTM cells after 24 h of OMD treatment at all three concentrations. Fig 1B shows the lack of cytotoxicity in all OMD-treated groups and only a slight increase (105.6%) in cell viability in the 10 nM OMD-treated group.

Effect of OMD on the mRNA expression of ECM in HTM cells

To investigate the effects of OMD on the mRNA expression of the ECM in HTM cells, the mRNA expression of fibronectin (*FN1*), collagen type I alpha 1 chain (*COL1A1*), collagen type

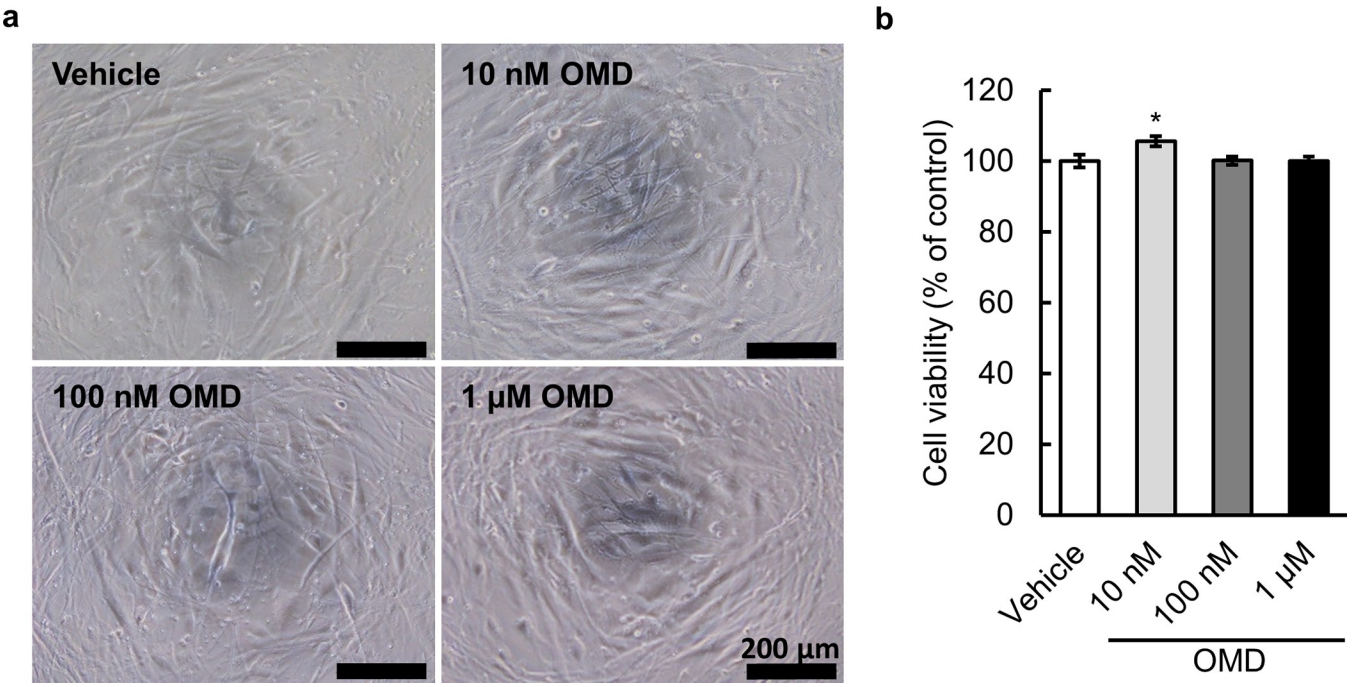

Fig 1. Effect of omidenepag (OMD) on human trabecular meshwork (HTM) cell viability. HTM cells were treated with vehicle or OMD (10 nM, 100 nM, and 1 μM) for 24 h, and cell viability was assessed using MTS assays. (**a**) Typical phase-contrast microscopic appearance of HTM cells after treatment. Scale bars = 200 μm. (**b**) Absorbance in each well was normalized to that in the vehicle-treated wells and presented as percentages. Each value represents the mean ± S.E. (n = 6). *$P < 0.05$, compared with the vehicle-treated group by Dunnett's multiple comparison test. MTS, 3-(4,5-dimethylthiazol-2-yl)-5-(3-carboxymethoxyphenyl)-2-(4-sulfophenyl)-2H-tetrazolium.

https://doi.org/10.1371/journal.pone.0280331.g001

I alpha 2 chain (*COL1A2*), collagen type IV alpha 2 chain (*COL4A2*), collagen type XII alpha 1 chain (*COL12A1*), collagen type XIII alpha 1 chain (*COL13A1*), and collagen type XVIII alpha 1 chain (*COL18A1*) was quantified using quantitative real-time PCR (Fig 2).

Under 2D culture conditions, the mRNA expression of *FN1*, *COL1A1*, *COL1A2*, *COL12A1*, and *COL13A1* was significantly downregulated in a concentration-dependent manner after 6 or 24 h of OMD treatment at all three concentrations. The results of all statistical analyses are shown in Table 2. *COL18A1* mRNA was significantly downregulated only after 6 h of treatment with 1 μM OMD. No significant changes in *COL4A2* mRNA expression were observed at any concentration or treatment period.

Under 3D culture conditions, *COL12A1* and *COL13A1* mRNA expression was significantly downregulated after 24 h treatment with OMD at all three concentrations, and *COL4A2* mRNA expression was significantly upregulated only when treated for 24 h with 1 μM OMD.

The mRNA expression of *FN1*, *COL1A1*, *COL1A2*, and *COL18A1* did not show significant changes at any concentration or treatment periods.

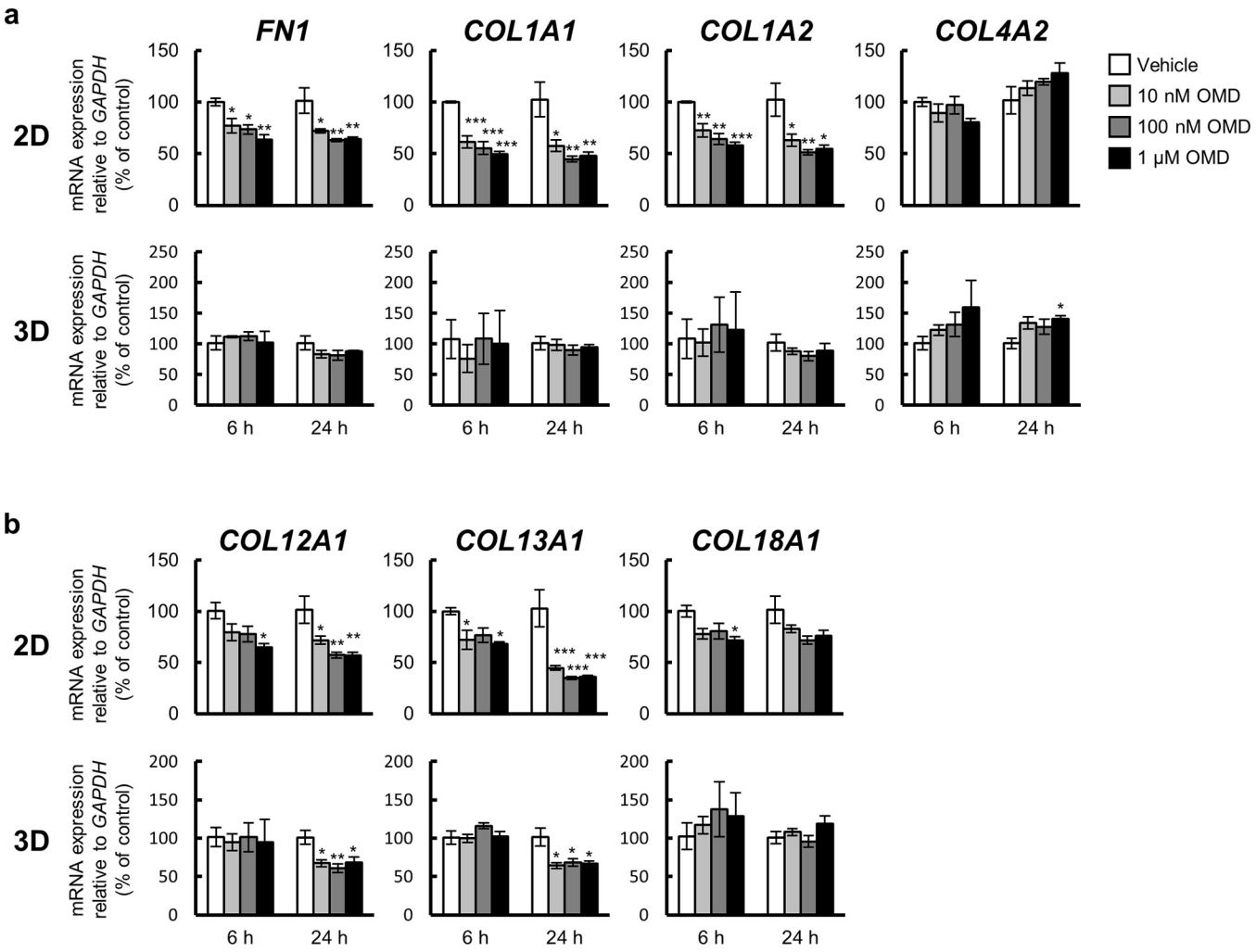

Fig 2. Effect of omidenepag (OMD) on extracellular matrix (ECM) gene expression in 2D- and 3D-cultured human trabecular meshwork (HTM) cells. 2D- or 3D-cultured HTM cells were treated with vehicle, 10 nM, 100 nM, or 1 μM OMD for 6 or 24 h, and the gene expression changes in ECMs [**(a)** *FN1*, *COL1A1*, *COL1A2*, and *COL4A2*, **(b)** *COL12A1*, *COL13A1*, and *COL18A1*] were assessed using quantitative real-time PCR. The mRNA expression level in each gene was normalized to that for *GAPDH* and presented as percentages relative to the vehicle-treated group. Each value represents the mean ± S.E. (n = 3). $^{*}P < 0.05$, $^{**}P < 0.01$, $^{***}P < 0.001$ compared with the vehicle-treated group by Dunnett's multiple comparison test.

https://doi.org/10.1371/journal.pone.0280331.g002

Table 2. P values for the gene expression changes in OMD-treated groups compared with the vehicle-treated group.

Gene	Culture condition	Treatment period (h)	Dunnett's test P value in OMD-treated group		
			10 nM	100 nM	1 μM
FN1	2D	6	0.0350*	0.0168*	0.0029**
		24	0.0135*	0.0019**	0.0025**
	3D	6	0.8557 (N.S.)	0.8229 (N.S.)	0.9997 (N.S.)
		24	0.2694 (N.S.)	0.2170 (N.S.)	0.5082 (N.S.)
COL1A1	2D	6	0.0007***	0.0003***	0.0001***
		24	0.0205*	0.0052**	0.0072**
	3D	6	0.8872 (N.S.)	1.0000 (N.S.)	0.9977 (N.S.)
		24	0.9896 (N.S.)	0.6746 (N.S.)	0.9056 (N.S.)
COL1A2	2D	6	0.0054**	0.0010**	0.0004***
		24	0.0316*	0.0083**	0.0116*
	3D	6	0.9992 (N.S.)	0.9615 (N.S.)	0.9902 (N.S.)
		24	0.6468 (N.S.)	0.3428 (N.S.)	0.7094 (N.S.)
COL4A2	2D	6	0.5600 (N.S.)	0.9754 (N.S.)	0.1669 (N.S.)
		24	0.6666 (N.S.)	0.3883 (N.S.)	0.1520 (N.S.)
	3D	6	0.8780 (N.S.)	0.7320 (N.S.)	0.3010 (N.S.)
		24	0.0792 (N.S.)	0.1682 (N.S.)	0.0409*
COL12A1	2D	6	0.1504 (N.S.)	0.1237 (N.S.)	0.0184*
		24	0.0492*	0.0070**	0.0067**
	3D	6	0.9891 (N.S.)	1.0000 (N.S.)	0.9906 (N.S.)
		24	0.0214*	0.0086**	0.0240*
COL13A1	2D	6	0.0295*	0.0638 (N.S.)	0.0146*
		24	0.0006***	0.0001***	0.0001***
	3D	6	0.9994 (N.S.)	0.2782 (N.S.)	0.9951 (N.S.)
		24	0.0124*	0.0223*	0.0172*
COL18A1	2D	6	0.0641 (N.S.)	0.1014 (N.S.)	0.0193*
		24	0.2628 (N.S.)	0.0579 (N.S.)	0.1040 (N.S.)
	3D	6	0.9582 (N.S.)	0.6716 (N.S.)	0.8248 (N.S.)
		24	0.8479 (N.S.)	0.9488 (N.S.)	0.3170 (N.S.)
MMP1	2D	6	0.1450 (N.S.)	0.1343 (N.S.)	0.0642 (N.S.)
		24	0.2284 (N.S.)	0.0311*	0.1921 (N.S.)
	3D	6	0.9975 (N.S.)	0.7227 (N.S.)	1.0000 (N.S.)
		24	0.0193*	0.0339*	0.0308*
MMP2	2D	6	0.1509 (N.S.)	0.2783 (N.S.)	0.0288*
		24	0.3088 (N.S.)	0.0735 (N.S.)	0.1498 (N.S.)
	3D	6	0.9989 (N.S.)	0.9810 (N.S.)	0.8508 (N.S.)
		24	0.6104 (N.S.)	0.2856 (N.S.)	0.0700 (N.S.)
MMP3	2D	6	0.0766 (N.S.)	0.0471*	0.0330*
		24	0.0697 (N.S.)	0.0183*	0.0601 (N.S.)
	3D	6	1.0000 (N.S.)	0.9980 (N.S.)	0.6673 (N.S.)
		24	0.9235 (N.S.)	0.1949 (N.S.)	0.1814 (N.S.)
MMP9	2D	6	0.2686 (N.S.)	0.1110 (N.S.)	0.0680 (N.S.)
		24	0.5568 (N.S.)	0.4209 (N.S.)	0.8833 (N.S.)
	3D	6	0.8561 (N.S.)	0.9977 (N.S.)	0.4209 (N.S.)
		24	0.9937 (N.S.)	0.8838 (N.S.)	0.9939 (N.S.)

(*Continued*)

Table 2. (Continued)

Gene	Culture condition	Treatment period (h)	Dunnett's test P value in OMD-treated group		
			10 nM	100 nM	1 μM
MMP11	2D	6	0.8584 (N.S.)	0.9900 (N.S.)	0.8662 (N.S.)
		24	0.8241 (N.S.)	0.9959 (N.S.)	0.7558 (N.S.)
	3D	6	0.0836 (N.S.)	0.1372 (N.S.)	0.8257 (N.S.)
		24	0.7044 (N.S.)	0.9992 (N.S.)	0.8420 (N.S.)
MMP12	2D	6	0.6537 (N.S.)	0.3020 (N.S.)	0.9571 (N.S.)
		24	0.0035**	0.0033**	0.0013**
	3D	6	0.9920 (N.S.)	0.9936 (N.S.)	0.6872 (N.S.)
		24	0.0918 (N.S.)	0.4956 (N.S.)	0.3962 (N.S.)
MMP14	2D	6	0.0001***	0.0001***	0.0000***
		24	0.1452 (N.S.)	0.0080**	0.0034**
	3D	6	0.9998 (N.S.)	0.9890 (N.S.)	0.6704 (N.S.)
		24	0.5992 (N.S.)	0.5110 (N.S.)	0.5357 (N.S.)
MMP15	2D	6	0.0289*	0.0156*	0.0053**
		24	0.0219*	0.0061**	0.0175*
	3D	6	0.9998 (N.S.)	0.8476 (N.S.)	0.2063 (N.S.)
		24	0.4737 (N.S.)	0.3173 (N.S.)	0.4516 (N.S.)
MMP16	2D	6	0.4794 (N.S.)	0.2708 (N.S.)	0.8713 (N.S.)
		24	0.0047**	0.0078**	0.0065**
	3D	6	0.9995 (N.S.)	0.9952 (N.S.)	0.9789 (N.S.)
		24	0.6542 (N.S.)	0.8057 (N.S.)	0.4501 (N.S.)
MMP17	2D	6	0.8188 (N.S.)	0.6390 (N.S.)	0.9981 (N.S.)
		24	0.7874 (N.S.)	0.4794 (N.S.)	0.4117 (N.S.)
	3D	6	0.8780 (N.S.)	0.8746 (N.S.)	0.3919 (N.S.)
		24	1.0000 (N.S.)	0.4254 (N.S.)	0.9999 (N.S.)
MMP24	2D	6	0.2069 (N.S.)	0.1283 (N.S.)	0.4015 (N.S.)
		24	0.0116*	0.0951 (N.S.)	0.0115*
	3D	6	0.9031 (N.S.)	0.2655 (N.S.)	0.9955 (N.S.)
		24	0.9036 (N.S.)	0.8347 (N.S.)	0.3973 (N.S.)
TIMP1	2D	6	0.0064**	0.0107*	0.0027**
		24	0.2134 (N.S.)	0.0877 (N.S.)	0.1495 (N.S.)
	3D	6	0.9998 (N.S.)	0.5857 (N.S.)	0.7965 (N.S.)
		24	0.9682 (N.S.)	0.3386 (N.S.)	0.5145 (N.S.)
TIMP2	2D	6	0.0230*	0.0205*	0.0094**
		24	0.0313*	0.0123*	0.0253*
	3D	6	0.9753 (N.S.)	0.7357 (N.S.)	0.6035 (N.S.)
		24	0.9619 (N.S.)	0.5219 (N.S.)	0.7236 (N.S.)
TIMP3	2D	6	0.5754 (N.S.)	0.7857 (N.S.)	0.9570 (N.S.)
		24	0.0481*	0.0021**	0.0003***
	3D	6	0.1230 (N.S.)	0.0529 (N.S.)	0.0180*
		24	0.0026**	0.0001***	0.0002***
TIMP4	2D	6	0.0695 (N.S.)	0.0350*	0.0086**
		24	0.0099**	0.0017**	0.0033**
	3D	6	0.9997 (N.S.)	0.7520 (N.S.)	0.9051 (N.S.)
		24	0.9963 (N.S.)	0.5939 (N.S.)	0.8105 (N.S.)

For each gene, the results of Dunnett's multiple comparison test are presented. n = 3 for each sample; P values indicate comparisons with the vehicle-treated group.

https://doi.org/10.1371/journal.pone.0280331.t002

In the 2D and 3D culture experiments, the shared gene expression changes were the downregulation of two ECM genes, *COL12A1* and *COL13A1*.

Effect of OMD on the mRNA expression of MMPs and TIMPs in HTM cells

To determine the effect of OMD on the mRNA expression of *MMPs* and *TIMPs* in HTM cells, that of *MMP1*, *MMP2*, *MMP3*, *MMP9*, *MMP11*, *MMP12*, *MMP14*, *MMP15*, *MMP16*, *MMP17*, and *MMP24*, and *TIMP1*, *TIMP2*, *TIMP3*, and *TIMP4* was quantified using quantitative real-time PCR (Figs 3 and 4).

Under 2D culture conditions, the mRNA expression of *MMP2* was significantly downregulated after 6 h, and that of *MMP1*, *MMP12*, *MMP16*, and *MMP24* was significantly downregulated after 24 h treatment with OMD (Fig 3). The mRNA expression of *MMP3* and *MMP15* was significantly downregulated after both 6 and 24 h of OMD treatment. *MMP14* mRNA expression was significantly downregulated after 6 h and upregulated after 24 h of OMD treatment. *TIMP1* mRNA expression was significantly downregulated following 6 h of OMD treatment and although it continued a downregulation trend, it was not significant 24 h post treatment (Fig 4). The mRNA expression of *TIMP2* and *TIMP4* was significantly downregulated after both 6 and 24 h of OMD treatment. *TIMP3* mRNA expression was significantly upregulated 24 h after treatment.

Under 3D culture conditions, *MMP1* mRNA expression was significantly downregulated 24 h after treatment, while *MMP11* appeared to be upregulated 6 h after treatment (Fig 3). No significant changes in mRNA expression of *TIMP1*, *TIMP2*, and *TIMP4* were observed at any concentration or treatment period (Fig 4). *TIMP3* mRNA expression was significantly upregulated after 6 and 24 h of treatment.

In the 2D and 3D culture experiments, the shared gene expression changes were the downregulation of *MMP1* (Fig 3) and upregulation of *TIMP3* (Fig 4).

Discussion

Owing to the limitations of 2D culture in evaluating drug efficacy, i.e., occasional inaccurate representation of tissue cells *in vitro* and different behaviors compared with those *in vivo*, 3D culture is being applied as an alternative to bridge the gap between 2D culture and animal models [38–40]. These are unique systems that can reflect cell–cell and cell–ECM interactions *in vivo* [41,42] and maintain their function and structure [43,44]. As for the TM tissue, it shows cell–ECM interactions and is involved in the regulation of aqueous humor dynamics because of its unique biomechanical properties [45,46]. Fibronectin is abundant in the TM tissue [47] where multiple subtypes of collagen (I, IV, XII, XVIII) are expressed [48–50]. MMP1, 2, 3, 9, 11, 12, 14, 15, 16, 17, and 24 are involved in the degradation of the ECM, while TIMPs suppress MMP activity by forming complexes with MMPs [51,52]. Considering these advantages, we used a 3D culture system that does not require specific scaffolds and is capable of constructing 3D tissue with uniform thickness, unlike spheroids [35], to evaluate the effects of OMD in the TM tissue *in vitro*.

In the present study, we evaluated the effects of OMD on the mRNA expression of the ECM, MMPs, and TIMPs in 2D- and 3D-cultured HTM cells, which have been confirmed to be TM cells that increase myocilin gene expression in response to steroids [31,32], in order to elucidate the IOP-lowering mechanism of OMDI that promotes the conventional outflow pathway.

According to the monkey pharmacokinetics data used for the new drug application of OMDI ophthalmic solution 0.002%, the OMD concentration in the TM tissue after instillation was estimated at 59.8 nM. Considering the agonistic activity of OMD to EP2 receptor (EC_{50} =

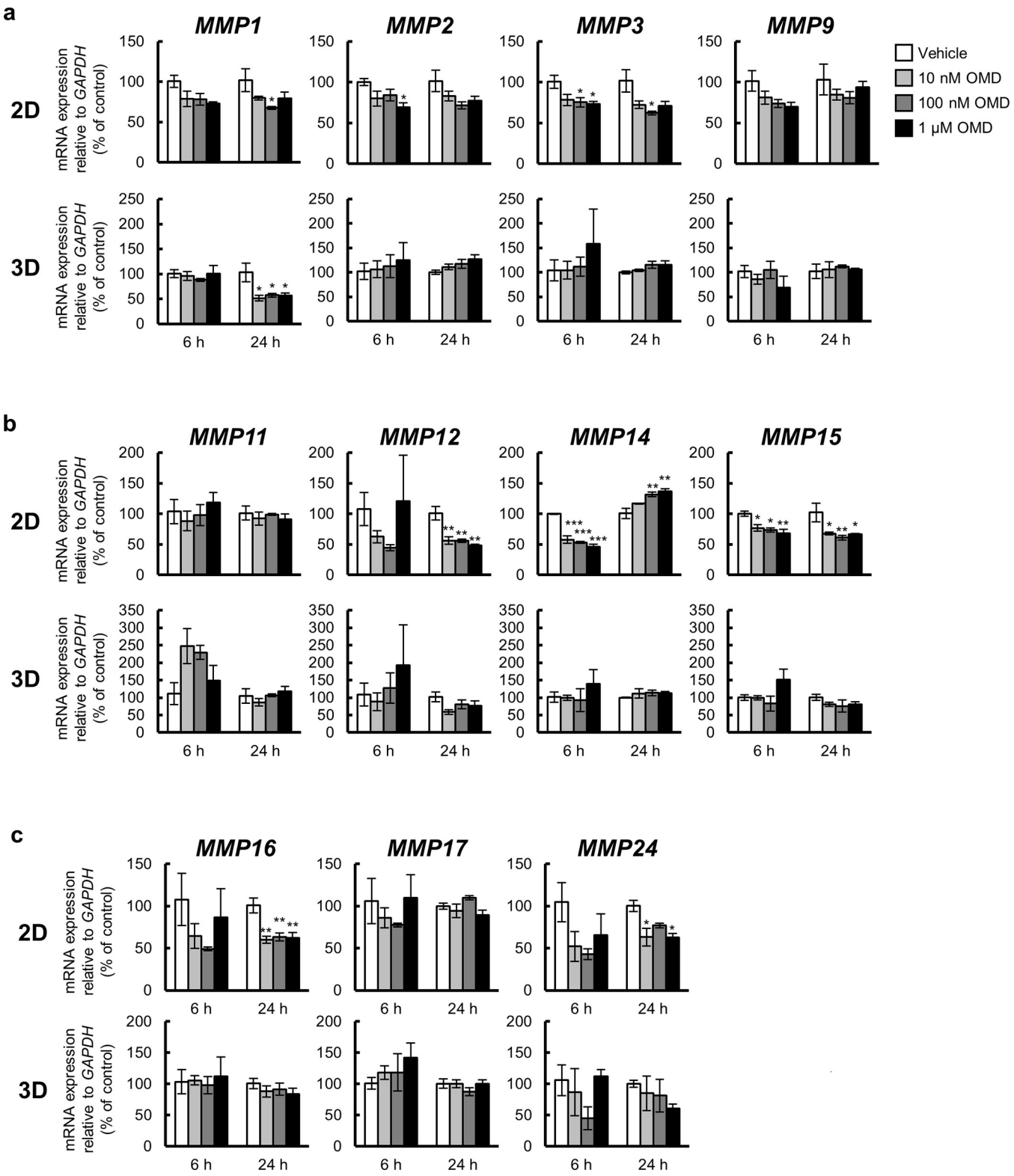

Fig 3. Effect of omidenepag (OMD) on matrix metalloproteinase (MMP) gene expression in 2D- and 3D-cultured human trabecular meshwork (HTM) cells. 2D- or 3D-cultured HTM cells were treated with vehicle, 10 nM, 100 nM, or 1 μM OMD for 6 or 24 h, and the gene expression changes of MMPs [**(a)** MMP1, MMP2, MMP3, and MMP9, **(b)** MMP11, MMP12, MMP14, and MMP15, **(c)** MMP16, MMP17, and MMP24] were assessed using quantitative real-time PCR; gene expression was assessed using real-time PCR. The mRNA expression level in each gene was normalized to that for *GAPDH* and presented as

percentages relative to the vehicle-treated group. Each value represents the mean ± S.E. (n = 3). $^{*}P < 0.05$, $^{**}P < 0.01$, $^{***}P < 0.001$ compared with the vehicle-treated group by Dunnett's multiple comparison test.

https://doi.org/10.1371/journal.pone.0280331.g003

8.3 nM), although a concentration range of 10–100 nM may be sufficient for evaluation, we extended the range from 10 nM to 1 μM in the present study. A significant increase in HTM cell viability was observed in the 10 nM OMD-treated group. However, the difference between the increase in cell viability in the vehicle-treated group and 10 nM OMD-treated group was only 5.6%, and no increase in HTM cell viability was observed at higher concentration rages (100 nM and 1 μM). Therefore, the increase in HTM cell viability in the 10 nM OMD-treated group was considered to be incidental and unrelated to cell proliferation.

Although 1 μM is higher than the estimated TM tissue concentrations in clinical practice, some genes with significant expression changes showed a concentration-dependent response within the concentration range of 10 nM to 1 μM (*FN1*, *COL1A1*, *COL1A2*, *COL12A1*, and *COL13A1*) in 2D culture. Conversely, among the genes that showed significant expression change in 3D culture, only *COL4A2* showed a significant expression change at 1 μM, and the other genes (*COL12A1*, *COL13A1*, *MMP1*, and *TIMP3*) showed significant expression changes from 10 nM to 1 μM. In clinical practice, the TM tissue is expected to be exposed to OMD at concentrations of approximately 50 nM. Further expression changes were observed at higher concentrations in 2D culture, while almost all responses to OMD in 3D culture reached a plateau at 10 nM, which may appropriately reflect the *in vivo* response to OMD after instillation.

These differences in expression between the 2D and 3D cultures may be attributed to changes in cellular response due to differences in culture environments. Drug sensitivity is increased in 2D culture systems [43], and hence the mRNA expression under the 2D culture condition may be overestimated. In addition, we have unpublished background data that indicate that the mRNA expression level of EP2 receptor in 2D-cultured HTM was higher than that of in 3D-cultured HTM; therefore, the increased drug sensitivity in 2D-cultured HTM was thought to be a plausible event. However, because such increased drug sensitivity under 2D culture conditions is useful for screening to broadly capture gene expression changes, we first evaluated the effect of OMD on HTM cells in 2D culture. Considering this, many changes

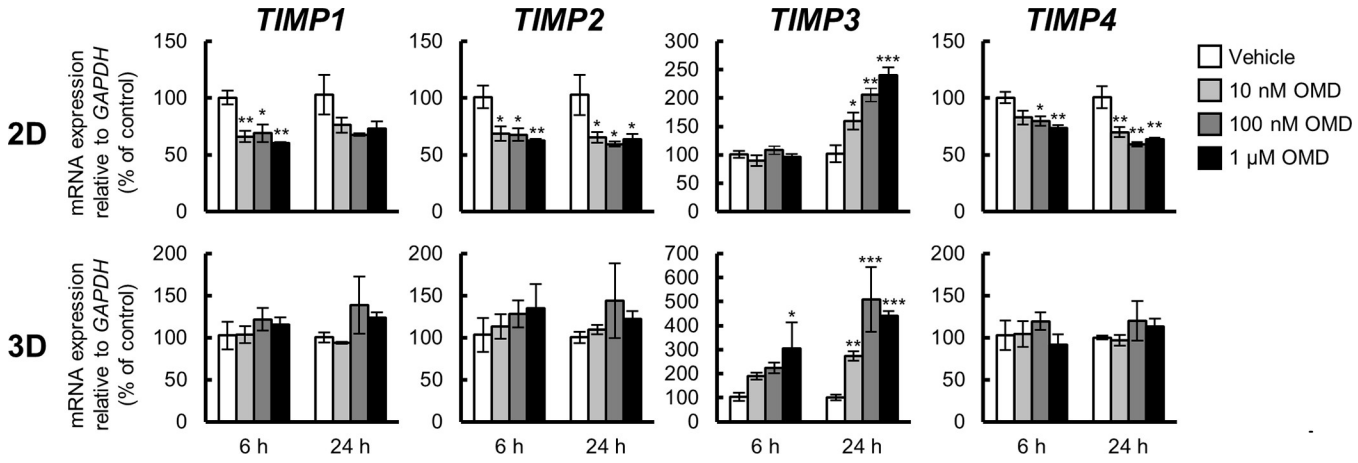

Fig 4. Effect of omidenepag (OMD) on tissue inhibitors of metalloproteinase (TIMP) gene expression in 2D- and 3D-cultured human trabecular meshwork (HTM) cells. 2D- or 3D-cultured HTM cells were treated with vehicle, 10 nM, 100 nM, or 1 μM OMD for 6 or 24 h, and the gene expression changes of TIMPs (*TIMP1*, *TIMP2*, *TIMP3*, and *TIMP4*) were assessed using quantitative real-time PCR. The mRNA expression level in each gene was normalized to that of *GAPDH* and presented as percentages relative to the vehicle-treated group. Each value represents the mean ± S.E. (n = 3). $^{*}P < 0.05$, $^{**}P < 0.01$, $^{***}P < 0.001$ compared with the vehicle-treated group by Dunnett's multiple comparison test.

https://doi.org/10.1371/journal.pone.0280331.g004

in mRNA expression were observed as described above. In contrast, the mRNA expression of only a few genes, such as *COL12A1* and *COL13A1*, was significantly downregulated under 3D culture conditions. Although we have not assessed the effect of OMD on collagen type XII and XIII proteins yet, the cellular responses to OMD in 3D culture conditions are expected to be similar to those *in vivo* because HTM cells under 3D culture conditions retain more cellular characteristics *in vivo* compared to 2D cultures.

Among the above gene expression changes, we hypothesized that downregulation of the ECM-related genes, especially *COL12A1* and *COL13A1*, might have caused the increase in aqueous humor outflow via the conventional outflow pathway followed by the decrease in IOP.

COL12 is a type of non-fibrillar collagen called fibril-associated collagens with interrupted triple helices (FACIT) that can form bonds between fibrils [49,53]. *COL12* expression increases in response to mechanical stimuli [54–57], while TM cells sense elevated IOP as a mechanical stretching [49]; hence, there is a possibility that COL12 expression and IOP might be correlated. Further, an EP2 receptor agonist (AH13205) has been found to contribute to the relaxation of isolated TM tissue [58]. Under the 3D culture conditions used in the present study, in addition to the direct downregulation by EP2 stimulation, the physical stimulus of TM relaxation by EP2 stimulation may also result in a significant downregulation of *COL12A1* expression. Based on these findings, it is possible that the IOP-lowering effect of OMDI is attributed to the reduction in aqueous humor outflow resistance caused by the physical relaxation of the TM tissue and reductions in mechanical stretching and *COL12* expression in TM tissue, which may contribute to ECM remodeling and consequently IOP reduction.

COL13 is a transmembrane collagen [59]. Its localization and function in the TM tissue and association with glaucoma are still unknown. However, *COL13* has cell adhesion-related functions at various cell–ECM junctions [60]. As the TM tissue is composed of TM cells and ECM, there is a possibility that *COL13* may be involved in cell–cell and cell–ECM adhesion of TM cells and the regulation of aqueous humor outflow resistance. Under this assumption, OMD downregulates *COL13A1* expression and consequently contributes to the reduction of aqueous humor outflow resistance in the TM tissue.

In the present study, *COL12A1* and *COL13A1* were downregulated following OMD treatment in 2D and 3D cultures. It is well known that reduced amount of ECM contributes to decreased outflow resistance [25,61–63]. Taken together, downregulation of those two genes may be one of the factors responsible for the IOP-lowering effect of OMDI.

However, there are certain limitations to this study. As the results in the present study were obtained from only one lot of HTM cells isolated from a single donor, they may be specific to this primary HTM cell alone; hence, further study might be necessary to evaluate whether the same results will be obtained using other HTM cells from other donors. Furthermore, we only evaluated gene expression using cell culture. Further studies to determine the effects of OMD on ECM protein expression and MMP activities under 3D culture conditions are currently underway. 3D-cultured tissue may reflect the TM tissue and the microenvironment of TM *in vivo* more accurately than 2D-cultured cells do. However, because the 3D cultured tissue does not fully reflect the *in vivo* TM structure, it should be noted that the results in the current study may not fully reproduce the *in vivo* TM response. As the accumulation of ECM in the TM tissue followed by increased conventional outflow resistance is an important factor that elevates IOP in glaucoma [24–26], suppression of ECM accumulation in the TM tissue is important for long-term IOP control in glaucoma treatment. Nonetheless, as OMDI suppresses the expression of *COL12A1* and *COL13A1*, which are part of the ECM components, OMDI could maintain the conventional outflow before ECM accumulation progresses and the TM tissue becomes completely occluded. Further clarification of the mechanism of OMDI in

the conventional outflow pathway may enhance its clinical use, such as administering OMDI when the conventional pathway is relatively healthier. In other words, OMDI may be feasibly administered when patients are still in earlier stages of glaucoma and have healthier TM tissue, thereby maintaining the conventional outflow. Such practices may enhance the use of OMDI among the many existing anti-glaucoma drugs in clinical practice.

Supporting information

S1 Fig. Effect of dexamethasone (DEX) on myocilin (MYOC) mRNA gene expression in HTM cells. HTM cells were seeded in 6-well plates pre-coated with poly-L-lysine at a density of 1.0×10^4 cells/well (1.1×10^3 cells/cm^2) and incubated for 24 h. Subsequently, these cells were treated with vehicle (TMCM with 0.01% DMSO) or 500 nM DEX for 6 d, and the changes in the gene expression of MYOC were assessed using quantitative real-time PCR. The mRNA expression level was normalized to that for GAPDH and presented as percentages relative to the vehicle-treated group. Each value represents the mean ± S.E. (n = 6). $^*P < 0.05$ compared with the vehicle-treated group by Student's t-test. The primer set for MYOC was predesigned and purchased from Takara Bio (Shiga, Japan; Cat. # HA205173).
(TIF)

S1 File. PCR data for S1 Fig.
(XLSX)

S2 File. MTS assay data for Fig 1.
(XLSX)

S3 File. PCR data for Fig 2A and 2B (2D).
(XLSX)

S4 File. PCR data for Fig 2A and 2B (3D).
(XLSX)

S5 File. PCR data for Fig 3A–3C (2D).
(XLSX)

S6 File. PCR data for Fig 3A–3C (3D).
(XLSX)

S7 File. PCR data for Fig 4 (2D).
(XLSX)

S8 File. PCR data for Fig 4 (3D).
(XLSX)

Acknowledgments

The authors would like to thank Ms. Naoko Yamashita for the excellent technical assistance.

Author Contributions

Conceptualization: Masashi Kumon, Masahiro Fuwa, Atsushi Shimazaki, Noriko Odani-Kawabata, Masatomo Kato.

Investigation: Masashi Kumon, Masahiro Fuwa.

Methodology: Masashi Kumon, Masahiro Fuwa.

Writing – original draft: Masashi Kumon, Masahiro Fuwa.

Writing – review & editing: Masashi Kumon, Masahiro Fuwa, Atsushi Shimazaki, Noriko Odani-Kawabata, Ryo Iwamura, Kenji Yoneda, Masatomo Kato.

References

1. Jonas JB, Aung T, Bourne RR, Bron AM, Ritch R, Panda-Jonas S. Glaucoma. The Lancet. 2017; 390 (10108):2183–93. https://doi.org/10.1016/s0140-6736(17)31469-1
2. Quigley HA. Glaucoma. Lancet. 2011; 377(9774):1367–77. Epub 20110330. https://doi.org/10.1016/S0140-6736(10)61423-7 PMID: 21453963; PubMed Central PMCID: PMC21453963.
3. Quigley HA, Broman AT. The number of people with glaucoma worldwide in 2010 and 2020. Br J Ophthalmol. 2006; 90(3):262–7. Epub 2006/02/21. https://doi.org/10.1136/bjo.2005.081224 PMID: 16488940; PubMed Central PMCID: PMC1856963.
4. Weinreb RN. Glaucoma neuroprotection: What is it? Why is it needed? Can J Ophthalmol. 2007; 42 (3):396–8. Epub 2007/05/18. https://doi.org/10.3129/canjophthalmol.i07-045 PMID: 17508033.
5. Collaborative Normal-Tension Glaucoma Study Group. The effectiveness of intraocular pressure reduction in the treatment of normal-tension glaucoma. Collaborative Normal-Tension Glaucoma Study Group. Am J Ophthalmol. 1998; 126(4):498–505. Epub 1998/10/21. https://doi.org/10.1016/s0002-9394(98)00272-4 PMID: 9780094.
6. Collaborative Normal-Tension Glaucoma Study Group. Comparison of glaucomatous progression between untreated patients with normal-tension glaucoma and patients with therapeutically reduced intraocular pressures. Am J Ophthalmol. 1998; 126(4):487–97. https://doi.org/10.1016/s0002-9394(98)00223-2
7. The AGIS Investigators. The Advanced Glaucoma Intervention Study (AGIS): 7. The relationship between control of intraocular pressure and visual field deterioration. Am J Ophthalmol. 2000; 130 (4):429–40. Epub 2000/10/12. https://doi.org/10.1016/s0002-9394(00)00538-9 PMID: 11024415.
8. Prum BE Jr., Lim MC, Mansberger SL, Stein JD, Moroi SE, Gedde SJ, et al. Primary Open-Angle Glaucoma Suspect Preferred Practice Pattern((R)) Guidelines. Ophthalmology. 2016; 123(1):P112–51. Epub 20151112. https://doi.org/10.1016/j.ophtha.2015.10.055 PMID: 26581560.
9. European Glaucoma Society Terminology and Guidelines for Glaucoma, 4th Edition—Chapter 3: Treatment principles and options Supported by the EGS Foundation: Part 1: Foreword; Introduction; Glossary; Chapter 3 Treatment principles and options. Br J Ophthalmol. 2017; 101(6):130–95. Epub 2017/06/01. https://doi.org/10.1136/bjophthalmol-2016-EGSguideline.003 PMID: 28559477; PubMed Central PMCID: PMC5583689.
10. Hollo G. The side effects of the prostaglandin analogues. Expert Opin Drug Saf. 2007; 6(1):45–52. Epub 2006/12/22. https://doi.org/10.1517/14740338.6.1.45 PMID: 17181451.
11. Alm A, Grierson I, Shields MB. Side effects associated with prostaglandin analog therapy. Surv Ophthalmol. 2008; 53 Suppl1:S93–105. Epub 2008/12/17. https://doi.org/10.1016/j.survophthal.2008.08.004 PMID: 19038628.
12. Cracknell KP, Grierson I. Prostaglandin analogues in the anterior eye: their pressure lowering action and side effects. Exp Eye Res. 2009; 88(4):786–91. Epub 20081002. https://doi.org/10.1016/j.exer.2008.08.022 PMID: 18930047.
13. Pharmaceuticals and Medical Devices Agency (PMDA). New Drugs Approved in FY 2018 2018 [cited 2022 March 29]. Available from: https://www.pmda.go.jp/files/000235288.pdf.
14. Santen Pharmaceutical Co., Ltd., Ube Industries, Ltd. Santen and Ube Industries Announce Receipt of Manufacturing and Marketing Approval for Glaucoma and Ocular Hypertension Treatment EYBELIS Ophthalmic Solution 0.002% in Japan [Internet]. 2018; September 21, 2018 [cited March 29, 2022]. Available from: https://ssl4.eir-parts.net/doc/4536/tdnet/1631167/00.pdf.
15. Kirihara T, Taniguchi T, Yamamura K, Iwamura R, Yoneda K, Odani-Kawabata N, et al. Pharmacologic Characterization of Omidenepag Isopropyl, a Novel Selective EP2 Receptor Agonist, as an Ocular Hypotensive Agent. Invest Ophthalmol Vis Sci. 2018; 59(1):145–53. Epub 2018/01/15. https://doi.org/10.1167/iovs.17-22745 PMID: 29332128.
16. Fuwa M, Shimazaki A, Odani-Kawabata N, Kirihara T, Taniguchi T, Iwamura R, et al. Additive Intraocular Pressure-Lowering Effects of a Novel Selective EP2 Receptor Agonist, Omidenepag Isopropyl, Combined with Existing Antiglaucoma Agents in Conscious Ocular Normotensive Monkeys. J Ocul Pharmacol Ther. 2021; 37(4):223–9. Epub 20210217. https://doi.org/10.1089/jop.2020.0071 PMID: 33600237.

17. Aihara M, Lu F, Kawata H, Iwata A, Liu K, Odani-Kawabata N, et al. Phase 2, Randomized, Dose-finding Studies of Omidenepag Isopropyl, a Selective EP2 Agonist, in Patients With Primary Open-angle Glaucoma or Ocular Hypertension. J Glaucoma. 2019; 28(5):375–85. Epub 2019/03/07. https://doi.org/10.1097/IJG.0000000000001221 PMID: 30839416.

18. Aihara M, Lu F, Kawata H, Iwata A, Odani-Kawabata N, Shams NK. Omidenepag Isopropyl Versus Latanoprost in Primary Open-Angle Glaucoma and Ocular Hypertension: The Phase 3 AYAME Study. Am J Ophthalmol. 2020; 220:53–63. Epub 20200610. https://doi.org/10.1016/j.ajo.2020.06.003 PMID: 32533949.

19. Aihara M, Ropo A, Lu F, Kawata H, Iwata A, Odani-Kawabata N, et al. Intraocular pressure-lowering effect of omidenepag isopropyl in latanoprost non-/low-responder patients with primary open-angle glaucoma or ocular hypertension: the FUJI study. Jpn J Ophthalmol. 2020; 64(4):398–406. Epub 20200622. https://doi.org/10.1007/s10384-020-00748-x PMID: 32572719.

20. Iwamura R, Tanaka M, Okanari E, Kirihara T, Odani-Kawabata N, Shams N, et al. Identification of a Selective, Non-Prostanoid EP2 Receptor Agonist for the Treatment of Glaucoma: Omidenepag and its Prodrug Omidenepag Isopropyl. J Med Chem. 2018; 61(15):6869–91. Epub 20180730. https://doi.org/10.1021/acs.jmedchem.8b00808 PMID: 29995405.

21. Yamamoto Y, Taniguchi T, Inazumi T, Iwamura R, Yoneda K, Odani-Kawabata N, et al. Effects of the Selective EP2 Receptor Agonist Omidenepag on Adipocyte Differentiation in 3T3-L1 Cells. J Ocul Pharmacol Ther. 2020; 36(3):162–9. Epub 20200114. https://doi.org/10.1089/jop.2019.0079 PMID: 31934812; PubMed Central PMCID: PMC7175626.

22. Esaki Y, Katsuta O, Kamio H, Noto T, Mano H, Iwamura R, et al. The Antiglaucoma Agent and EP2 Receptor Agonist Omidenepag Does Not Affect Eyelash Growth in Mice. J Ocul Pharmacol Ther. 2020; 36(7):529–33. Epub 20200517. https://doi.org/10.1089/jop.2020.0003 PMID: 32412835; PubMed Central PMCID: PMC7482127.

23. Fuwa M, Toris CB, Fan S, Taniguchi T, Ichikawa M, Odani-Kawabata N, et al. Effects of a Novel Selective EP2 Receptor Agonist, Omidenepag Isopropyl, on Aqueous Humor Dynamics in Laser-Induced Ocular Hypertensive Monkeys. J Ocul Pharmacol Ther. 2018; 34(7):531–7. Epub 20180710. https://doi.org/10.1089/jop.2017.0146 PMID: 29989843.

24. Johnson M. 'What controls aqueous humour outflow resistance?'. Exp Eye Res. 2006; 82(4):545–57. Epub 20060104. https://doi.org/10.1016/j.exer.2005.10.011 PMID: 16386733; PubMed Central PMCID: PMC2892751.

25. Acott TS, Kelley MJ. Extracellular matrix in the trabecular meshwork. Exp Eye Res. 2008; 86(4):543–61. Epub 20080125. https://doi.org/10.1016/j.exer.2008.01.013 PMID: 18313051; PubMed Central PMCID: PMC2376254.

26. Acott TS, Vranka JA, Keller KE, Raghunathan V, Kelley MJ. Normal and glaucomatous outflow regulation. Prog Retin Eye Res. 2021; 82:100897. Epub 20200811. https://doi.org/10.1016/j.preteyeres.2020.100897 PMID: 32795516; PubMed Central PMCID: PMC7876168.

27. Coleman AL, Miglior S. Risk factors for glaucoma onset and progression. Surv Ophthalmol. 2008; 53 Suppl1:S3–10. Epub 2008/12/17. https://doi.org/10.1016/j.survophthal.2008.08.006 PMID: 19038621.

28. Weinreb RN, Toris CB, Gabelt BT, Lindsey JD, Kaufman PL. Effects of prostaglandins on the aqueous humor outflow pathways. Surv Ophthalmol. 2002; 47 Suppl 1:S53–64. Epub 2002/09/03. https://doi.org/10.1016/s0039-6257(02)00306-5 PMID: 12204701.

29. Nilsson SF, Drecoll E, Lutjen-Drecoll E, Toris CB, Krauss AH, Kharlamb A, et al. The prostanoid EP2 receptor agonist butaprost increases uveoscleral outflow in the cynomolgus monkey. Invest Ophthalmol Vis Sci. 2006; 47(9):4042–9. Epub 2006/08/29. https://doi.org/10.1167/iovs.05-1627 PMID: 16936121.

30. Nakamura N, Honjo M, Yamagishi R, Igarashi N, Sakata R, Aihara M. Effects of selective EP2 receptor agonist, omidenepag, on trabecular meshwork cells, Schlemm's canal endothelial cells and ciliary muscle contraction. Sci Rep. 2021; 11(1):16257. Epub 20210810. https://doi.org/10.1038/s41598-021-95768-z PMID: 34376747; PubMed Central PMCID: PMC8355290.

31. Inoue-Mochita M, Inoue T, Fujimoto T, Kameda T, Awai-Kasaoka N, Ohtsu N, et al. p38 MAP kinase inhibitor suppresses transforming growth factor-beta2-induced type 1 collagen production in trabecular meshwork cells. PLoS One. 2015; 10(3):e0120774. Epub 20150323. https://doi.org/10.1371/journal.pone.0120774 PMID: 25799097; PubMed Central PMCID: PMC4370581.

32. Diskin S, Chen WS, Cao Z, Gyawali S, Gong H, Soza A, et al. Galectin-8 promotes cytoskeletal rearrangement in trabecular meshwork cells through activation of Rho signaling. PLoS One. 2012; 7(9):e44400. Epub 20120904. https://doi.org/10.1371/journal.pone.0044400 PMID: 22973445; PubMed Central PMCID: PMC3433423.

33. Ahadome SD, Zhang C, Tannous E, Shen J, Zheng JJ. Small-molecule inhibition of Wnt signaling abrogates dexamethasone-induced phenotype of primary human trabecular meshwork cells. Exp Cell Res.

2017; 357(1):116–23. Epub 20170517. https://doi.org/10.1016/j.yexcr.2017.05.009 PMID: 28526237; PubMed Central PMCID: PMC5535738.

34. Keller KE, Bhattacharya SK, Borras T, Brunner TM, Chansangpetch S, Clark AF, et al. Consensus recommendations for trabecular meshwork cell isolation, characterization and culture. Exp Eye Res. 2018; 171:164–73. Epub 20180309. https://doi.org/10.1016/j.exer.2018.03.001 PMID: 29526795; PubMed Central PMCID: PMC6042513.

35. Tanaka HY, Kitahara K, Sasaki N, Nakao N, Sato K, Narita H, et al. Pancreatic stellate cells derived from human pancreatic cancer demonstrate aberrant SPARC-dependent ECM remodeling in 3D engineered fibrotic tissue of clinically relevant thickness. Biomaterials. 2019; 192:355–67. Epub 20181117. https://doi.org/10.1016/j.biomaterials.2018.11.023 PMID: 30476717.

36. Sasaoka M, Ota T, Kageyama M. Rotenone-induced inner retinal degeneration via presynaptic activation of voltage-dependent sodium and L-type calcium channels in rats. Sci Rep. 2020; 10(1):969. Epub 20200122. https://doi.org/10.1038/s41598-020-57638-y PMID: 31969611; PubMed Central PMCID: PMC6976703.

37. Taniguchi T, Endo KI, Tanioka H, Sasaoka M, Tashiro K, Kinoshita S, et al. Novel use of a chemically modified siRNA for robust and sustainable in vivo gene silencing in the retina. Sci Rep. 2020; 10 (1):22343. Epub 20201218. https://doi.org/10.1038/s41598-020-79242-w PMID: 33339841; PubMed Central PMCID: PMC7749170.

38. Jensen C, Teng Y. Is It Time to Start Transitioning From 2D to 3D Cell Culture? Front Mol Biosci. 2020; 7:33. Epub 20200306. https://doi.org/10.3389/fmolb.2020.00033 PMID: 32211418; PubMed Central PMCID: PMC7067892.

39. Habanjar O, Diab-Assaf M, Caldefie-Chezet F, Delort L. 3D Cell Culture Systems: Tumor Application, Advantages, and Disadvantages. Int J Mol Sci. 2021; 22(22). Epub 20211111. https://doi.org/10.3390/ijms222212200 PMID: 34830082; PubMed Central PMCID: PMC8618305.

40. Fontoura JC, Viezzer C, Dos Santos FG, Ligabue RA, Weinlich R, Puga RD, et al. Comparison of 2D and 3D cell culture models for cell growth, gene expression and drug resistance. Mater Sci Eng C Mater Biol Appl. 2020; 107:110264. Epub 20191014. https://doi.org/10.1016/j.msec.2019.110264 PMID: 31761183.

41. Kim JB. Three-dimensional tissue culture models in cancer biology. Semin Cancer Biol. 2005; 15 (5):365–77. https://doi.org/10.1016/j.semcancer.2005.05.002 PMID: 15975824.

42. Godugu C, Patel AR, Desai U, Andey T, Sams A, Singh M. AlgiMatrix based 3D cell culture system as an in-vitro tumor model for anticancer studies. PLoS One. 2013; 8(1):e53708. Epub 20130118. https://doi.org/10.1371/journal.pone.0053708 PMID: 23349734; PubMed Central PMCID: PMC3548811.

43. Bokhari M, Carnachan RJ, Cameron NR, Przyborski SA. Culture of HepG2 liver cells on three dimensional polystyrene scaffolds enhances cell structure and function during toxicological challenge. J Anat. 2007; 211(4):567–76. Epub 20070815. https://doi.org/10.1111/j.1469-7580.2007.00778.x PMID: 17711423; PubMed Central PMCID: PMC2375833.

44. Vernazza S, Tirendi S, Scarfi S, Passalacqua M, Oddone F, Traverso CE, et al. 2D- and 3D-cultures of human trabecular meshwork cells: A preliminary assessment of an in vitro model for glaucoma study. PLoS One. 2019; 14(9):e0221942. Epub 20190906. https://doi.org/10.1371/journal.pone.0221942 PMID: 31490976; PubMed Central PMCID: PMC6731014.

45. Vranka JA, Kelley MJ, Acott TS, Keller KE. Extracellular matrix in the trabecular meshwork: intraocular pressure regulation and dysregulation in glaucoma. Exp Eye Res. 2015; 133:112–25. https://doi.org/10.1016/j.exer.2014.07.014 PMID: 25819459; PubMed Central PMCID: PMC4379427.

46. Maddala R, Rao PV. Global phosphotyrosinylated protein profile of cell-matrix adhesion complexes of trabecular meshwork cells. Am J Physiol Cell Physiol. 2020; 319(2):C288–C99. Epub 20200520. https://doi.org/10.1152/ajpcell.00537.2019 PMID: 32432933; PubMed Central PMCID: PMC7500213.

47. Faralli JA, Filla MS, Peters DM. Role of Fibronectin in Primary Open Angle Glaucoma. Cells. 2019; 8 (12). Epub 20191126. https://doi.org/10.3390/cells8121518 PMID: 31779192; PubMed Central PMCID: PMC6953041.

48. Rehnberg M, Ammitzboll T, Tengroth B. Collagen distribution in the lamina cribrosa and the trabecular meshwork of the human eye. Br J Ophthalmol. 1987; 71(12):886–92. https://doi.org/10.1136/bjo.71.12.886 PMID: 3426993; PubMed Central PMCID: PMC1041338.

49. Keller KE, Kelley MJ, Acott TS. Extracellular matrix gene alternative splicing by trabecular meshwork cells in response to mechanical stretching. Invest Ophthalmol Vis Sci. 2007; 48(3):1164–72. https://doi.org/10.1167/iovs.06-0875 PMID: 17325160.

50. Ohlmann AV, Ohlmann A, Welge-Lussen U, May CA. Localization of collagen XVIII and endostatin in the human eye. Curr Eye Res. 2005; 30(1):27–34. https://doi.org/10.1080/02713680490894333 PMID: 15875362.

51. Weinreb RN, Robinson MR, Dibas M, Stamer WD. Matrix Metalloproteinases and Glaucoma Treatment. J Ocul Pharmacol Ther. 2020; 36(4):208–28. Epub 20200401. https://doi.org/10.1089/jop.2019.0146 PMID: 32233938; PubMed Central PMCID: PMC7232675.

52. Lee HJ, Kim YH, Choi DW, Cho KA, Park JW, Shin SJ, et al. Tonsil-derived mesenchymal stem cells enhance allogeneic bone marrow engraftment via collagen IV degradation. Stem Cell Res Ther. 2021; 12(1):329. Epub 20210605. https://doi.org/10.1186/s13287-021-02414-6 PMID: 34090520; PubMed Central PMCID: PMC8180137.

53. September AV, Posthumus M, van der Merwe L, Schwellnus M, Noakes TD, Collins M. The COL12A1 and COL14A1 genes and Achilles tendon injuries. Int J Sports Med. 2008; 29(3):257–63. Epub 20071025. https://doi.org/10.1055/s-2007-965127 PMID: 17960519.

54. Arai K, Nagashima Y, Takemoto T, Nishiyama T. Mechanical strain increases expression of type XII collagen in murine osteoblastic MC3T3-E1 cells. Cell Struct Funct. 2008; 33(2):203–10. Epub 20081029. https://doi.org/10.1247/csf.08025 PMID: 18957791.

55. Trachslin J, Koch M, Chiquet M. Rapid and reversible regulation of collagen XII expression by changes in tensile stress. Exp Cell Res. 1999; 247(2):320–8. https://doi.org/10.1006/excr.1998.4363 PMID: 10066359.

56. Fluck M, Tunc-Civelek V, Chiquet M. Rapid and reciprocal regulation of tenascin-C and tenascin-Y expression by loading of skeletal muscle. J Cell Sci. 2000; 113 (Pt 20):3583–91. https://doi.org/10.1242/jcs.113.20.3583 PMID: 11017874.

57. Karimbux NY, Nishimura I. Temporal and spatial expressions of type XII collagen in the remodeling periodontal ligament during experimental tooth movement. J Dent Res. 1995; 74(1):313–8. https://doi.org/10.1177/00220345950740010501 PMID: 7876423.

58. Stumpff F, Boxberger M, Krauss A, Rosenthal R, Meissner S, Choritz L, et al. Stimulation of cannabinoid (CB1) and prostanoid (EP2) receptors opens BKCa channels and relaxes ocular trabecular meshwork. Exp Eye Res. 2005; 80(5):697–708. Epub 20050104. https://doi.org/10.1016/j.exer.2004.12.003 PMID: 15862177.

59. Peltonen S, Hentula M, Hagg P, Yla-Outinen H, Tuukkanen J, Lakkakorpi J, et al. A novel component of epidermal cell-matrix and cell-cell contacts: transmembrane protein type XIII collagen. J Invest Dermatol. 1999; 113(4):635–42. https://doi.org/10.1046/j.1523-1747.1999.00736.x PMID: 10504453.

60. Hägg P, Väisänen T, Tuomisto A, Rehn M, Tu H, Huhtala P, et al. Type XIII collagen: a novel cell adhesion component present in a range of cell–matrix adhesions and in the intercalated discs between cardiac muscle cells. Matrix Biol. 2001; 19(8):727–42. https://doi.org/10.1016/s0945-053x(00)00119-0 PMID: 11223332

61. Wallace DM, Murphy-Ullrich JE, Downs JC, O'Brien CJ. The role of matricellular proteins in glaucoma. Matrix Biol. 2014; 37:174–82. Epub 20140412. https://doi.org/10.1016/j.matbio.2014.03.007 PMID: 24727033.

62. Fleenor DL, Shepard AR, Hellberg PE, Jacobson N, Pang IH, Clark AF. TGFbeta2-induced changes in human trabecular meshwork: implications for intraocular pressure. Invest Ophthalmol Vis Sci. 2006; 47(1):226–34. https://doi.org/10.1167/iovs.05-1060 PMID: 16384967.

63. Fan Y, Wei J, Guo L, Zhao S, Xu C, Sun H, et al. Osthole Reduces Mouse IOP Associated With Ameliorating Extracellular Matrix Expression of Trabecular Meshwork Cell. Invest Ophthalmol Vis Sci. 2020; 61(10):38. https://doi.org/10.1167/iovs.61.10.38 PMID: 32821914; PubMed Central PMCID: PMC7445364.